

Reorientation of Aquaporin-1 Topology during Maturation in the Endoplasmic Reticulum

Yun Lu,^{*†} Isaiah R. Turnbull,^{*} Alvina Bragin,[‡] Kristin Carveth,^{*} A.S. Verkman,[§] and William R. Skach^{*||}

^{*}Molecular Medicine Division, Oregon Health Sciences University, Portland, Oregon 97201;

[‡]Department of Medicine, University of Pennsylvania, Philadelphia, Pennsylvania 19104; and

[§]Cardiovascular Research Unit, University of California, San Francisco, California 94143

Submitted October 14, 1999; Revised May 4, 2000; Accepted June 19, 2000

Monitoring Editor: Chris Kaiser

The topology of most eukaryotic polytopic membrane proteins is established cotranslationally in the endoplasmic reticulum (ER) through a series of coordinated translocation and membrane integration events. For the human aquaporin water channel AQP1, however, the initial four-segment-spanning topology at the ER membrane differs from the mature six-segment-spanning topology at the plasma membrane. Here we use epitope-tagged AQP1 constructs to follow the transmembrane (TM) orientation of key internal peptide loops in *Xenopus* oocyte and cell-free systems. This analysis revealed that AQP1 maturation in the ER involves a novel topological reorientation of three internal TM segments and two peptide loops. After the synthesis of TMs 4–6, TM3 underwent a 180-degree rotation in which TM3 C-terminal flanking residues were translocated from their initial cytosolic location into the ER lumen and N-terminal flanking residues underwent retrograde translocation from the ER lumen to the cytosol. These events convert TM3 from a type I to a type II topology and reposition TM2 and TM4 into transmembrane conformations consistent with the predicted six-segment-spanning AQP1 topology. AQP1 topological reorientation was also associated with maturation from a protease-sensitive conformation to a protease-resistant structure with water channel function. These studies demonstrate that initial protein topology established via cotranslational translocation events in the ER is dynamic and may be modified by subsequent steps of folding and/or maturation.

INTRODUCTION

The biogenesis of polytopic membrane proteins in the endoplasmic reticulum (ER) involves the proper positioning of transmembrane (TM) helices, coordinated folding of cytosolic and luminal peptide domains, and helical packing within the lipid bilayer. One model predicts that protein topology is established through cotranslational translocation and integration events as the nascent chain emerges from the ribosome (Blobel, 1980; Rapoport *et al.*, 1996; Johnson, 1997). During this process, signal sequences target the nascent chain to the ER, facilitate ribosome binding to the Sec61 translocation complex (translocon), and open a large aqueous channel in the ER membrane through which the nascent

polypeptide moves (Simon and Blobel, 1991; Crowley *et al.*, 1994; Jungnickel and Rapoport, 1995; Mothes *et al.*, 1997). Stop-transfer sequences subsequently terminate translocation, close the translocon, disrupt the ribosome–membrane junction, and direct the polypeptide laterally into the lipid bilayer (Yost *et al.*, 1983; Do *et al.*, 1996; Liao *et al.*, 1997; Mothes *et al.*, 1997). By regulating ribosome binding and translocon gating, signal and stop-transfer sequences are thereby able to direct specific regions of the elongating nascent chain into the cytosol or ER lumen and to coordinate the sequential orientation and integration of multiple TM segments (Rothman *et al.*, 1988; Wessels and Spiess, 1988; Lipp *et al.*, 1989).

In recent years, it has become evident that certain naturally occurring polytopic proteins exhibit variations in biogenesis that do not follow a simple cotranslational model (Hegde and Lingappa, 1997; Johnson, 1997). First, signal sequences that direct translocation of N-terminal flanking residues may result in the posttranslational positioning of peptide loops and/or TM segments (Lu *et al.*, 1997; Ota *et al.*, 1998). Second, certain topogenic determinants terminate translocation but fail to integrate into the membrane, sug-

[†] Present address: Genetics and Biochemistry Branch, National Institutes of Health, Bethesda, MD 20892.

^{||} Corresponding author. E-mail address: skachw@ohsu.edu.
Abbreviations used: AQP, aquaporin; CRM, canine rough microsomes; ER, endoplasmic reticulum; PK, proteinase K; RRL, rabbit reticulocyte lysate; TM, transmembrane; XO, *Xenopus laevis* oocytes; XOmb, *Xenopus* oocyte-derived ER membranes.

gesting that TM segments may coassemble within or near the translocon before fully entering the lipid bilayer (Audigier *et al.*, 1987; Skach and Lingappa, 1993; Skach *et al.*, 1994; Lin and Addison, 1995; Borel and Simon, 1996). Third, the correct positioning of TM segments may require the synthesis of distal C-terminal peptide regions, indicating that initial translocation events may not necessarily dictate the topology of the mature protein (Wilkinson *et al.*, 1996). Thus, to predict the effects of structural determinants on topological outcome, it will be necessary to define different topogenic pathways through which polytopic proteins acquire their specific topology (Hegde and Lingappa, 1997; Johnson, 1997; Bibi, 1998).

Previously, we examined the biogenesis of two related proteins, aquaporin-1 (AQP1/CHIP28) and aquaporin-4 (AQP4/MIWC), and showed that they use markedly different folding pathways to acquire their transmembrane topology at the ER membrane (Skach *et al.*, 1994; Shi *et al.*, 1995). AQP1 and AQP4 are ~70% homologous, and each contains six predicted TM segments that form a water-selective pore in biological membranes (Hasegawa *et al.*, 1994; Verkman *et al.*, 1996; Agre *et al.*, 1998). Analysis of sequentially truncated AQP4 fusion proteins demonstrated that the six-segment-spanning (six-spanning) AQP4 topology was established through a series of cotranslational translocation and integration events by alternating signal and stop-transfer sequences (Shi *et al.*, 1995). In contrast, a parallel analysis revealed that topogenic determinants encoded within AQP1 cotranslationally directed a topology with only four TM segments (Skach *et al.*, 1994). This latter finding was particularly unexpected because mature AQP1 at the plasma membrane contains six TM segments, as originally predicted (Preston and Agre, 1991; Preston *et al.*, 1994; Cheng *et al.*, 1997; Walz *et al.*, 1997). These results suggested either that the majority of AQP1 is synthesized in a misfolded (i.e. four-spanning) conformation that is degraded before reaching the plasma membrane or, alternatively, that AQP1 maturation involves an unusual topological reorientation to achieve its six-spanning topology.

To determine the relationship between the four-spanning and six-spanning AQP1 structures, we analyzed a series of AQP1 constructs containing two separate translocation reporters and followed the dynamic topology of internal TM segments as a function of nascent chain length. We now show that AQP1 maturation proceeds through a complex folding pathway that involves at least three distinct steps: cotranslational formation of a transient four-spanning topology, topological rearrangement of internal TM segments into a loosely folded six-spanning topology, and final compaction of the transmembrane core to a protease-resistant conformation. These studies thus identify an unexpected level of complexity in polytopic protein biogenesis and demonstrate that the initial protein topology at the ER membrane is dynamic and may be modified by subsequent steps of folding and/or maturation.

MATERIALS AND METHODS

cDNA Constructs

Plasmid pSP64.CHIP28 (Skach *et al.*, 1994) was used as the template for PCR amplifications to generate myc-tagged AQP1 constructs. *Bst*EII restriction sites were inserted into pSP64.CHIP28 at codons

P77 and T120 with overlapping sense and antisense oligonucleotides (Ho *et al.*, 1989). A synthetic oligonucleotide encoding the c-myc epitope, 9E10 (Evan *et al.*, 1985), with compatible 5' overlapping *Bst*EII ends was ligated into these sites to generate plasmids AQP1.P77.myc and AQP1.T120.myc. The resulting sequence (verified by DNA sequencing) encoded the following amino acid residues:

AQP1.P77.myc	LNP-VT-EQKLISEEDL-VT-TLG
AQP1.T120.myc	SLT-VT-EQKLISEEDL-VT-GNS

where VT represents codons inserted by the *Bst*EII restriction site, and EQKLISEEDL represents the myc epitope. Plasmids T120.myc.TM3^T, -TM4^T, -TM5^T, and -TM6^T were generated by ligating an *Aval* fragment from previously described CHIP28 clones 6, 7, 8, and 9, respectively (Skach *et al.*, 1994), into the AQP1.T120.myc plasmid digested with *Aval*. These plasmids encode the AQP1 coding sequence up to residues L139, P169, V214, or V264, respectively, followed by a 142-residue C-terminal fragment of bovine prolactin (P) described previously (Rothman *et al.*, 1988). The locations of the myc epitope and the C-terminal fusion sites in these constructs are shown schematically in Figure 1. AQP1 fusion proteins containing the P reporter at residues R93, V107, and L139 were described previously (Skach *et al.*, 1994). Plasmid AQP1.T120.P (containing the P reporter fused to AQP1 residue T120) was generated by PCR amplification of pSP64.CHIP28 with the use of sense oligonucleotide, SP6 promoter, and antisense oligonucleotide AAGCGAGGT-CACCGTCAGGGAGGAGGTGAT. PCR fragments were digested with *Nco*I and *Bst*EII and ligated upstream of the P reporter in an *Nco*I-*Bst*EII-digested vector, S.L.ST.gG.P, as described previously (Skach and Lingappa, 1994). Plasmid myc.AQP1 was generated by digesting pSP64.CHIP28 with *Nco*I (at the ATG start codon) and ligating synthetic oligonucleotides with compatible overlapping ends encoding the myc epitope. The resulting N-terminal sequence encoded residues MEQKLISEEDL-M.

In Vitro Transcription/Translation

mRNA was transcribed with SP6 RNA polymerase (New England Biolabs, Beverly, MA) in a 10- μ l volume at 40°C for 1 h, as described previously (Skach *et al.*, 1994). Aliquots were used immediately or frozen in liquid nitrogen and stored at -80°C. The transcription mixture was added directly to the translation mixture containing [³⁵S]methionine (Tran³⁵S-label, ICN Pharmaceuticals, Irvine, CA) and 40% rabbit reticulocyte lysate (RRL), and translation was carried out for 1 h at 24°C under conditions described previously (Skach, 1998). Microsomal membranes prepared from dog pancreas (Walter and Blobel, 1983) were added to a final concentration of A₂₈₀ = 8.0 at the start of translation. In experiments in which oocyte membranes were used, 200- μ l aliquots of frozen membranes (prepared as described below) were quickly thawed, diluted with 0.3 volume of 90 mM KCl, 50 mM HEPES, pH 7.1, and spun at 10,000 \times g for 10–15 min at 4°C. Supernatant was removed in its entirety, and the pellet (~2 μ l volume) was resuspended directly into 18 μ l of translation mixture. Translation was then carried out as described above. For pulse-chase experiments, translation was terminated after 1 h by the addition of cycloheximide (0.5 mM), and samples were incubated at 24°C for the indicated times.

Xenopus laevis Oocyte Expression

For functional studies, plasmids were linearized with *Bam*HI and transcribed in vitro, and transcript mixture was injected directly into defolliculated stage V or VI *Xenopus laevis* oocytes as described (Zhang and Verkman, 1991). For topology and protein analysis, 50 μ Ci of [³⁵S]methionine (0.5 μ l of a 10 \times concentrated Tran³⁵S-label [ICN Pharmaceuticals]) was added to 2 μ l of transcription mixture and injected into stage VI *Xenopus* oocytes (50 nl/oocyte) on ice. After incubation at 18°C in modified Barth's solution [MBS; 88 mM NaCl, 1 mM KCl, 2.4 mM NaHCO₃, 0.82 mM MgSO₄, 0.33 mM

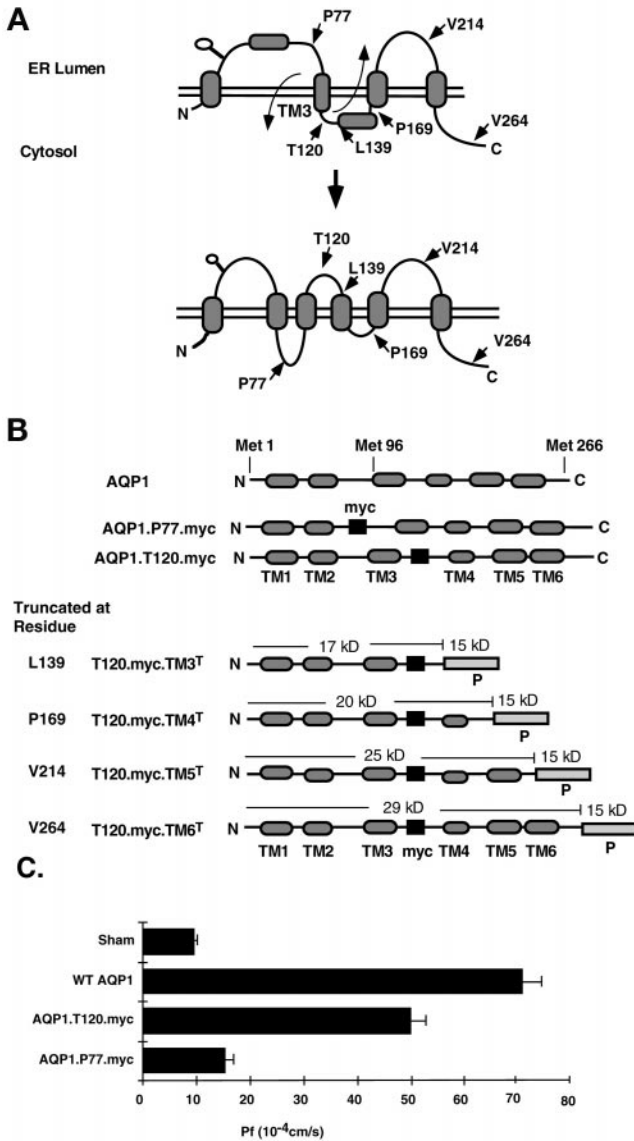


Figure 1. (A) Diagram of initial AQP1 four-spanning ER topology and mature six-spanning plasma membrane topology. Shaded ovals represent TM segments and open circles represent the glycosylation site at residue N42. Curved arrows indicate the predicted 180-degree rotation of TM3 required for maturation from the four-spanning to the six-spanning structure. Straight arrows indicate the site and topological orientation of the P reporter for fusion proteins at indicated truncation sites. (B) Scheme of epitope-tagged AQP1 constructs indicating the relative locations of myc and P reporters. Black rectangles represent the myc epitope tag and hatched rectangles represent the P reporter. Predicted masses of myc-tagged truncated polypeptides are indicated. (C) Water permeability (P_f) of oocytes injected with water or cRNA encoding wild-type AQP1, AQP1.T120.myc, and AQP1.P77.myc. Results represent the average of two separate experiments, six oocytes per group, mean \pm SE.

Ca(NO₃)₂, 0.41 mM CaCl₂, 10 mM sodium HEPES, pH 7.4], oocytes were homogenized on ice in 10 volumes of 0.25 M sucrose, 50 mM acetate, 5 mM Mg acetate, 1.0 mM DTT, 50 mM Tris, pH 7.5, with the

use of a Teflon hand-held homogenizer. Under these conditions, synthesis of radiolabeled constructs required a minimum of 60–90 min, and proteolysis was performed at a time of maximal synthesis when polypeptides were localized to the ER compartment (our unpublished results). For pulse-chase experiments, *Xenopus* oocytes were incubated for 1.5–3 h in MBS and then chased in MBS containing 2 mM methionine to prevent further incorporation of radioisotope (Xiong *et al.*, 1997).

Oocyte Water Permeability

Oocyte water permeability was determined 24–48 h after injection with the use of a swelling assay (Zhang and Verkman, 1991). The time course of swelling was measured in response to a 20-fold dilution of the extracellular Barth's buffer with distilled water. Oocyte volume was measured in 1-s intervals by quantitative imaging. Temperature control was maintained by a circulating water bath. Oocyte water permeability (P_f) was calculated from the initial rate of swelling [$d(V/V_0)/dt$] by the relation:

$$P_f = [d(V/V_0)/dt]/[(S/V_0)V_w(Osm_{out} - Osm_{in})],$$

where $S/V_0 = 50 \text{ cm}^{-1}$, $V_w = 18 \text{ cm}^3/\text{mol}$, and $Osm_{out} - Osm_{in} = 190 \text{ mOsm}$.

Preparation of *Xenopus* Oocyte Membranes

Xenopus laevis oocytes (XO) membranes were prepared as described by Kobilka (1990) with some modification. Stage VI *Xenopus* oocytes were surgically harvested, dissected, and treated with collagenase (type IV, 2 mg/ml; Sigma Chemical, St. Louis, MO) at room temperature for 45 min. Oocytes were rinsed five times with 5 volumes of 90 mM KCl, 50 mM HEPES, pH 7.1. Buffer was replaced with 40% sucrose (wt/vol) in 90 mM KCl, 50 mM HEPES, pH 7.1, equal to the volume of the oocytes. All subsequent steps were carried out at 0–4°C. The oocytes were gently broken by passing the mixture through an 18-gauge 1.5-inch needle 10 times. The homogenate was then centrifuged for 3 min at 3000 $\times g$. The supernatant was transferred to a new tube, and the process was repeated five times. The resulting milky white supernatant, containing cytosol and membranes, was divided into 200- μ l aliquots, frozen in liquid nitrogen, and stored at -80°C.

Protease Digestion

Protease digestion was performed as described previously (Skach *et al.*, 1994). Translation mixture or XO homogenate was divided into aliquots on ice, and CaCl₂ was added to 10 mM final concentration. Proteinase K (PK) was then added (0.2 mg/ml final concentration) in the presence or absence of 1% Triton X-100. Samples were incubated on ice for 1 h, and residual protease was inactivated by rapid mixing with PMSF (10 mM) and boiling in 10 volumes of 1% SDS, 0.1 M Tris, pH 8.0, for 5 min. Samples were then diluted in >10 volumes of buffer A (0.1 M NaCl, 1% Triton X-100, 2 mM EDTA, 0.1 mM PMSF, 0.1 M Tris, pH 8.0). RRL samples were immunoprecipitated directly. XO samples were incubated at 4°C for 1–2 h and centrifuged at 16,000 $\times g$ for 15 min to remove insoluble debris before immunoprecipitation. Accuracy of the protease protection assay was regularly assessed with the use of a secretory control protein. Only experiments in which protection of the control was consistently >85% were used. Because protease protection was typically 90–95% efficient, the actual translocation efficiency of aquaporin constructs is likely slightly higher than the calculated values.

Immunoprecipitation and Immunoabsorption

For immunoprecipitation, anti-prolactin antiserum (ICN Biomedicals, Costa Mesa, CA) or mAb myc-9E10 (Evan *et al.*, 1985) (mouse ascites) at 1:1000 dilution was added to translation products solu-

bilized in buffer A. After 10–30 min of preincubation, 5.0 μ l of protein A–Affigel (Bio-Rad, Richmond, CA) was added, and samples were rotated at 4°C for 10 h before washing three times with buffer A and twice with 0.1 M NaCl, 0.1 M Tris, pH 8.0, and addition of SDS sample buffer.

For immunoadsorption, translation products were layered onto 0.5 M sucrose, 100 mM KCl, 5.0 mM MgCl₂, 1.0 mM DTT, 50 mM HEPES, pH 7.5, and centrifuged at 180,000 \times g for 10 min at 4°C. The membrane pellet was resuspended in 50 μ l of ice-cold 0.1 M sucrose, 0.1 M KCl, 5 mM MgCl₂, 1 mM DTT, 50 mM HEPES, pH 7.5, and diluted into 0.5 ml of 0.1 M NaCl, 0.1 M Tris, pH 8.0, in the presence (immunoadsorption) or absence (immunoprecipitation) of antibody. Aliquots were incubated at 4°C for 2 h and centrifuged at 16,000 \times g for 30 min, and pellets were dissolved in buffer A. Protein A–Affigel (5 μ l) was added to each tube, and antibody was added to the immunoprecipitation tube. Subsequent steps were the same as those described for immunoprecipitation.

Autoradiography and Quantitation

Samples were analyzed by SDS-PAGE (EN³HANCE, Dupont/New England Nuclear, Boston, MA), fluorography, and autoradiography. Autoradiograms were quantitated with the use of a Pharmacia LKB (Piscataway, NJ) Image Master DTS densitometer (and/or phosphorimaging) and quantitated with the use of Image Master 1D software version 1.0 (Pharmacia LKB). Before analysis, the densitometer was precalibrated with a Kodak (Rochester, NY) photographic step tablet (0.2-OD intervals) to correct for film nonlinearity (0.07–1.8 OD units). The linearity of densitometry was confirmed by multiple timed exposures of serially diluted translation products over a 40-fold concentration range and by direct comparison with phosphorimaging analysis with the use of a Bio-Rad Personal Molecular Imager Fx (Kodak screens, Quant-1 software). Band intensities were calculated based on the volume averaged pixel intensity (OD \times mm²) of autoradiograms and/or by direct phosphorimaging of gels. Translocation efficiencies were determined by correcting for the fractional methionine content remaining in the protease-protected peptide fragments relative to starting materials. AQP1 contains three methionine residues at positions 1, 96, and 266 (Figure 1). The P reporter contains four methionine residues. Except as noted, the calculated translocation efficiencies represent the sum of the indicated fragments in which the reporter epitope was protected in the absence of detergent. Figures were prepared from representative autoradiograms with the use of an AGFA (Gruciert, NV) Studio Scan II transmission scanner and Adobe (Mountain View, CA) Photoshop software.

RESULTS

Construction of Epitope-tagged AQP1 Fusion Proteins

C-terminal translocation reporters are increasingly being used to study the biogenesis and topology of prokaryotic and eukaryotic polytopic integral membrane proteins (Boyd *et al.*, 1990; Broome-Smith *et al.*, 1990; Chavez and Hall, 1992; Traxler *et al.*, 1993; Skach *et al.*, 1994; Beja and Bibi, 1995; Shi *et al.*, 1995; Whale and Stoffel, 1996; Schmidt-Rose and Jentsch, 1997; Ota *et al.*, 1998). In this technique, the nascent chain is sequentially truncated and ligated to a reporter domain, and the orientation of the reporter relative to the membrane is used to infer the topology of the fusion site. By analyzing a series of such fusion proteins, it is possible to define the topology of the nascent chain at specific stages of protein synthesis and to localize topogenic determinants that initiate and terminate translocation. Because each construct provides topological information at only one fusion

site and because residues downstream of the fusion site are deleted, the resulting topology reflects only those translocation events that are directed by upstream, i.e., N-terminal, topogenic determinants. This is not a problem for proteins that acquire their topology cotranslationally. However, it has important implications if the initial cotranslational topology differs from the topology of the mature protein.

Topological analyses have previously demonstrated that the initial topology of AQP1 at the ER membrane contains four TM segments and three extramembranous peptide loops, whereas the mature protein at the plasma membrane contains six TM segments connected by five peptide loops (Preston *et al.*, 1994; Skach *et al.*, 1994). Experimental differences in AQP1 topology are primarily limited to the transmembrane orientation of TM3 and its flanking residues (Figure 1A). In particular, TM3 N-terminal and C-terminal flanking residues are initially directed into the ER lumen and cytosol, respectively, during AQP1 synthesis (Skach *et al.*, 1994), but they reside in the opposite orientation on functionally mature AQP1 molecules (Preston *et al.*, 1994). The hypothesis of this study is that AQP1 maturation involves a 180-degree rotation of TM3 from its initial type I topology to its mature type II topology. Such a rotation would properly position TM3 flanking residues and also orient TM2 and TM4 into their final transmembrane orientations without altering the topology of other regions of the protein (Figure 1A).

To monitor TM3 topology, a 10-residue c-myc epitope tag (Evan *et al.*, 1985) was engineered into either the TM3-TM4 peptide loop at residue T120 or within the TM2-TM3 peptide loop at position P77 of AQP1 (Figure 1B). The resulting plasmids (AQP1.T120.myc and AQP1.P77.myc) were then sequentially truncated at residues L139, P169, V214, or V264 after TM segments 3, 4, 5, and 6, respectively, and fused to a passive C-terminal translocation reporter (P) derived from bovine prolactin (Rothman *et al.*, 1988). The predicted sizes of truncated, myc-tagged AQP1 polypeptides are indicated in Figure 1B. The P reporter, which encodes 142 C-terminal residues from the secretory protein bovine prolactin, has a molecular mass of ~15 kDa.

If TM3 reoriented from a type I to a type II topology, then the myc epitope at position T120 would translocate from the cytosol to the ER lumen, whereas the epitope at position P77 would move from the ER lumen back into the cytosol (Figure 1A). Reorientation of TM3 flanking residues would thus serve as a marker for conversion of AQP1 from a four-spanning to a six-spanning topology, because this would also likely bring TM2 and TM4 into their proper membrane-spanning orientations (Figure 1). By simultaneously characterizing the protease accessibility of myc and P reporters in nascent chains of increasing length, we reasoned that it should be possible to define the point, either during or after AQP1 synthesis, at which such reorientation occurs.

Effect of Epitope Insertion on AQP1 Function

To determine whether the presence of the myc epitope grossly altered AQP1 folding, we first expressed full-length AQP1.T120.myc and AQP1.P77.myc proteins in XO, which are known to efficiently synthesize functional water channels (Zhang and Verkman, 1991; Preston *et al.*, 1992). Oocytes were microinjected with wild-type or myc-tagged AQP1 cRNA, and plasma membrane water permeability

was determined by osmotically induced swelling. As shown in Figure 1C, AQP1.T120.myc exhibited nearly 70% of wild-type AQP1 water channel activity. This is consistent with the findings of Preston *et al.* (1994) that T120 is a permissive site for epitope insertion. In contrast, myc insertion in the TM2-TM3 peptide loop (AQP1.P77.myc) resulted in very poor expression and rapid degradation of AQP1 (our unpublished results) and nearly complete disruption of water channel activity (Figure 1C). For these reasons, initial experiments focused on the T120 myc-tagged constructs.

Topology of AQP1 in *Xenopus Oocytes*

The cotranslational topology of TM3 was confirmed with the use of a series of fusion proteins in which the C-terminal P reporter was engineered into native AQP1 at residues N terminal (R93) or C terminal (V107, T120, or L139) to TM3. cRNA was coinjected with [³⁵S]methionine into mature XO, and after 2 h, oocytes were homogenized, digested with PK in the presence and absence of nondenaturing detergent, and immunoprecipitated with anti-prolactin antiserum. Under these conditions, synthesis of radiolabeled protein required 60–90 min, and proteolysis was performed before significant degradation at the time of maximal synthesis while constructs remained in the ER compartment (Xiong *et al.*, 1997; our unpublished results). Each construct generated nonglycosylated and core-glycosylated protein consistent with previous studies (Skach *et al.*, 1994) (Figure 2, lanes 1, 4, 7, and 10; the glycosylation site at residue N42 is indicated in the diagram). Glycosylation was verified by endoglycosidase H digestion and/or in vitro translation in the presence and absence of microsomal membranes (Skach *et al.*, 1994; our unpublished results). Protease digestion revealed that the P reporter was translocated into the ER lumen (i.e., protected from protease) in >85% of polypeptides when fused N terminal to TM3 at residue R93. In this construct, glycosylated and nonglycosylated polypeptides both yielded protease-protected bands (Figure 2, lanes 1–3). As noted previously (Skach *et al.*, 1994), some nascent chains also underwent a cleavage event, presumably by signal peptidase, to generate an additional protease-protected, 16-kDa peptide fragment. When the P reporter was fused at positions C terminal to TM3, it was degraded by PK in 85–95% of chains (lanes 4–12). A small amount of protease resistance was observed for these constructs that could represent either incomplete digestion or translocation of the reporter in a minor fraction (<15%) of chains. Together, these data demonstrate that before synthesis of TM4, TM3 initially spans the XO ER membrane in a type I topology with its N terminus flanking residues in the ER lumen and its C-terminal residues in the cytosol. The location of each fusion site flanking TM3 in the deduced topology is shown in Figure 2. The initial topology of TM1 and TM2 is also shown as determined in previous studies (Skach *et al.*, 1994).

We next used myc-tagged plasmids T120.myc.TM3^T, T120.myc.TM4^T, T120.myc.TM5^T, and T120.myc.TM6^T (truncated at residues L139, P169, V214, and V264, respectively) or full-length AQP1.T120.myc to determine whether TM3 remained in a type I orientation during the remainder of AQP1 synthesis. Constructs were again labeled with [³⁵S]methionine in microinjected XO, digested with PK, and immunoprecipitated with either anti-myc or anti-P antiserum before SDS-PAGE. As shown in Figure 3A, the myc

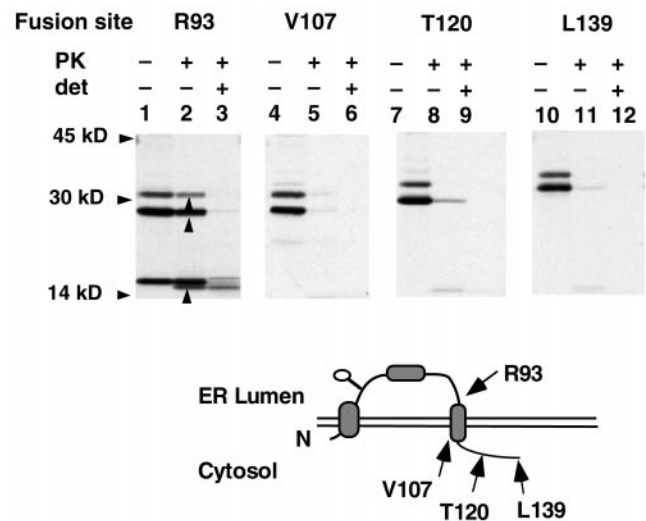


Figure 2. Cotranslational topology of TM3 in XO. AQP1 was truncated and fused to the C-terminal P reporter at residues R93, V107, T120, and L139 as indicated. Oocytes expressing in vitro transcribed cRNA were homogenized, digested with PK, and immunoprecipitated with anti-prolactin antiserum. Upward arrowheads (lane 2) indicate PK-protected, P-reactive fragments. The topological location of the P reporter in each fusion protein is shown in the diagram beneath the autoradiograms. In lane 3, a small amount of protease-resistant material was recovered in the presence of detergent. This is observed in some experiments and likely represents protein that, for unclear reasons, has become intrinsically resistant to PK digestion.

tag at residue T120 did not change the initial type I orientation of TM3. Nascent chains were glycosylated (at residue N42) as indicated, and both the myc and P reporters remained predominantly in the cytosol and accessible to protease. After synthesis of TM4 (plasmid T120.myc.TM4^T), the C-terminal P reporter remained cytosolic and PK accessible (Figure 3B). Immunoprecipitation with myc antiserum recovered a faint fragment 16 kDa in size (Figure 3B, lane 2). (Fragments were better appreciated upon longer exposure [our unpublished results].) Although this fragment exhibits only 6% of the intensity of the starting material in lane 1, it is predicted to contain 33% of methionine residues encoded within the intact fusion protein. Two methionine residues likely remain in the AQP1 fragment (M1 and M96). Four methionine residues in the P reporter are digested. (Note the absence of P-reactive fragments in lane 5.) M1 is not removed by PK because the 17-residue cytosolic N terminus of AQP1 is sterically inaccessible (Skach *et al.*, 1994). Therefore, after synthesis of TM4, the myc epitope became protected from protease in a minor fraction (~20%) of nascent chains.

For the T120.myc.TM5^T construct, truncated at residue V214, the P reporter was translocated into the ER lumen (Figure 3C). Translocation efficiency of the P reporter varied somewhat between experiments but was ~50% (average of three experiments), consistent with the known signal sequence activity encoded within TM5. This resulted in partial glycosylation of residue N205 in addition to residue N42 and the appearance of three full-length protein bands (Figure 3C, lanes 1 and 4), as described previously (Skach *et al.*, 1994). Fifteen percent to 20% of nascent chains were com-

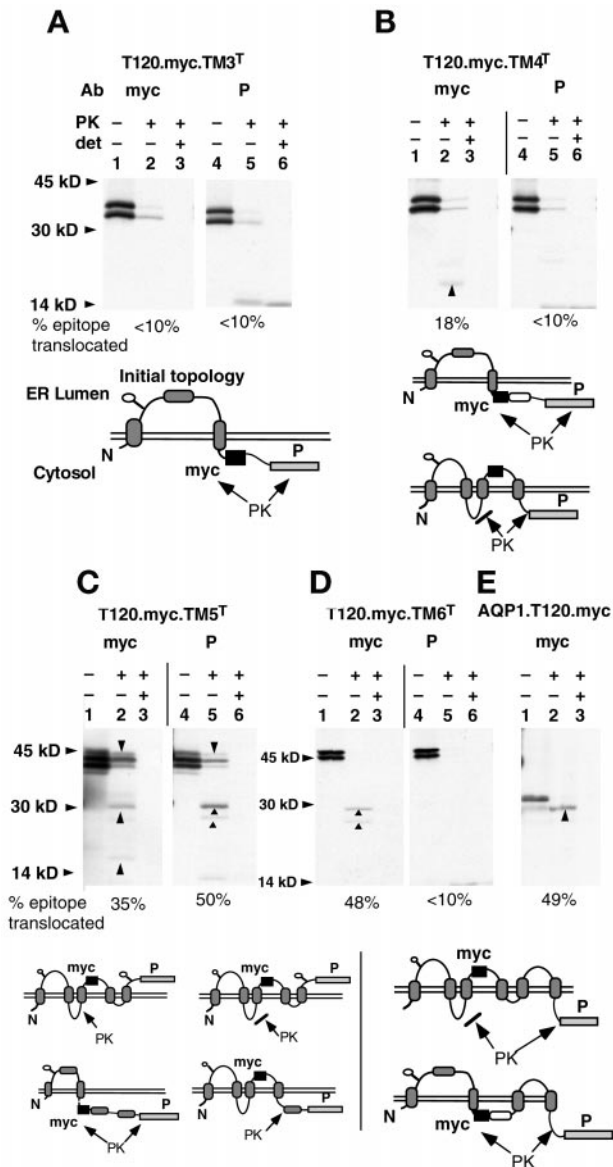


Figure 3. Topological reorientation of TM3 in XO. Plasmids encoding the myc reporter at AQP1 residue T120 and the P reporter after TM3, TM4, TM5, or TM6 as indicated (A–D, respectively) were expressed in XO and digested with PK in the presence or absence of Triton X-100 (det) as described in MATERIALS AND METHODS. Samples were immunoprecipitated with anti-myc (myc) or anti-prolactin (P) antiserum and analyzed by SDS-PAGE. (E) Results for full-length AQP1.T120.myc. Upward arrowheads (B–E) indicate PK-protected polypeptide fragments generated by protease digestion. Downward arrowheads (C) indicate full-length chains in which cytosolic loops are not accessible to protease. Diagrams beneath each autoradiogram indicate potential topologies of myc and P epitopes deduced by PK digestion. Sites of PK digestion are indicated by arrows, whereas inaccessible sites are indicated by arrows blocked by lines. The topologies of myc and P reporters are derived from the accessibility of epitopes based on patterns of protected fragments.

pletely resistant to PK digestion in the absence of detergent (Figure 3C, downward arrowheads). Thus, the myc epitope was inaccessible in these polypeptides. PK digestion also generated several myc-reactive, protease-protected fragments (Figure 3C, lane 2, upward arrowheads). Interestingly, a 30-kDa fragment was reactive to both P and myc antibodies (Figure 3C, lanes 2 and 5, upward arrowheads). Because the P reporter is 15 kDa in size, this fragment likely resulted from PK digestion at the N terminus of TM3 (the predicted cleavage site is diagrammed in Figure 3C). This would remove 10–12 kDa of AQP1 polypeptide and generate a fragment containing the P reporter plus an additional 15 kDa of glycosylated, myc-tagged AQP1 polypeptide. These fragments represent 10% of the initial signal and contain five of the six methionine residues present in full-length chains. A smaller myc-reactive fragment, 16 kDa in size, was also observed that represented 2% of the initial signal but contained only 33% of the initial methionine residues (Figure 3C, lane 2). The presence of these heterogeneous fragments suggests that several alternative topological forms exist in the ER membrane at this particular stage of AQP1 biogenesis (Figure 3C). Based on the predicted methionine distribution in the fusion protein, we calculate that the myc epitope became protected from protease in 35% of nascent chains immediately after synthesis of TM5.

Protease digestion of the T120.myc.TM6^T construct generated two myc-reactive polypeptide fragments of 29 and 26 kDa (Figure 3D, upward arrowheads). In this case, the shift in size was due to removal of the P reporter and cytosolic AQP1 C-terminal residues in glycosylated and unglycosylated polypeptides, respectively (note the absence of P-protected fragments in Figure 3D, lane 5). Protected fragments represent 16% of the initial band intensity but contain only 33% of the initial methionine residues. Therefore, the myc epitope was protected in 48% of total chains synthesized. Similarly, 49% of chains derived from the full-length AQP1.T120.myc construct also generated a 29-kDa myc-reactive core fragment after PK digestion. This is consistent with PK digestion within the 42-residue AQP1 C-terminal cytosolic domain (Figure 3E). The protected fragments in each of these constructs thus represent the entire hydrophobic core of AQP1, which together with the myc tag and N-linked oligosaccharide has a predicted size of ~29 kDa.

These results indicate that in XO, synthesis of AQP1-TM4, -TM5, and -TM6 was associated with partial reorientation of the TM3-TM4 peptide loop from its initial protease-accessible, cytosolic location to a protease-protected, detergent-sensitive site, presumably in the ER lumen.

In Vitro AQP1 Topology

AQP1 achieves a cotranslational four-spanning topology when expressed in RRL supplemented with canine pancreas microsomal membranes (CRM) (Skach *et al.*, 1994). Therefore, we tested whether AQP1 topological maturation was also reconstituted in vitro. Plasmids T120.myc.TM4^T, -TM5^T, and -TM6^T and full-length AQP1.T120.myc were expressed in RRL supplemented with CRM, and reporter topology was determined by protease digestion and immunoprecipitation (Figure 4A). Each construct generated core-glycosylated protein similar to that observed in XO. In CRM, the P reporter was completely digested by PK when engineered after TMs 4 and 6 (Figure 4A, lanes 4–6 and 16–18, respec-

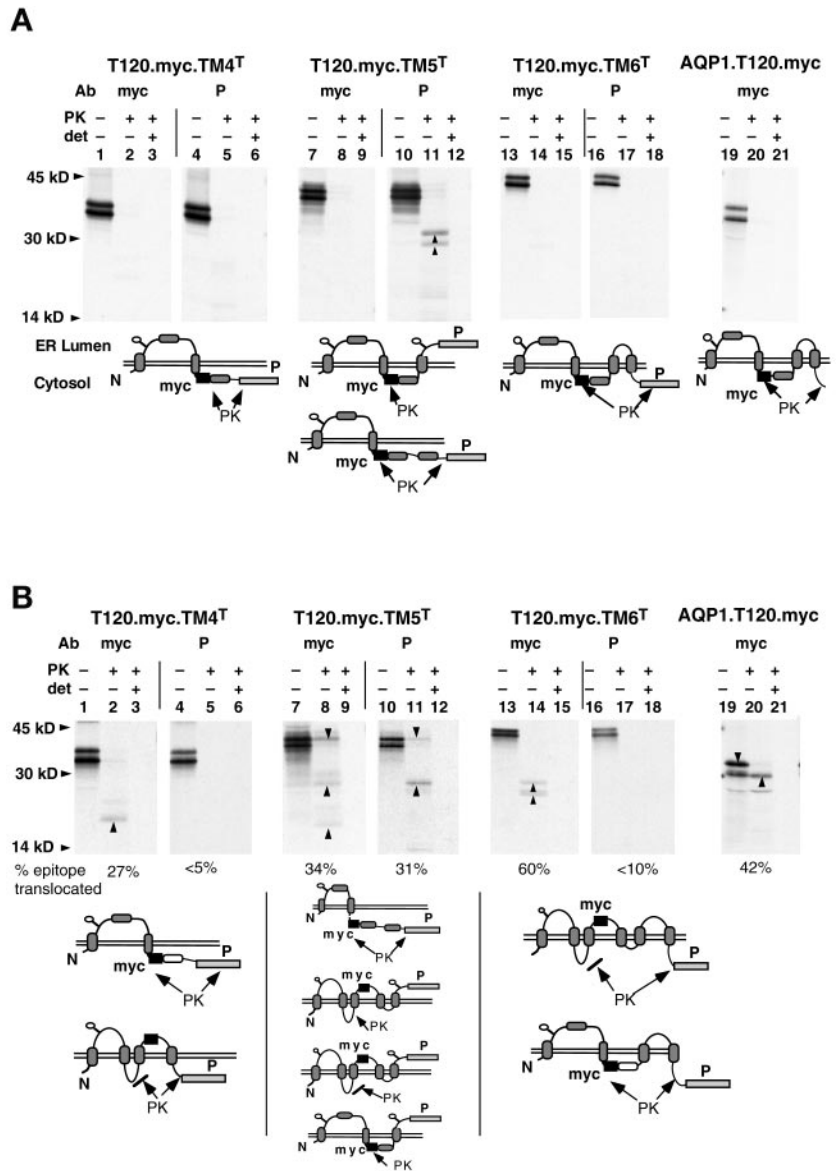


Figure 4. In vitro AQP1 topology. Expression of T120.myc.TM4^T, -TM5^T, and -TM6^T and AQP1.T120.myc in RRL and canine pancreas microsomes (A) or oocyte-derived ER membranes (B). Translation products were digested with PK and immunoprecipitated as in Figure 3. Upward arrowheads indicate polypeptide fragments protected from PK digestion in the absence, but not in the presence, of detergent. Potential topologies of epitopes indicated beneath autoradiograms are deduced from the protease accessibility of myc and P reporters. Sites of PK digestion are indicated.

tively). When the reporter followed TM5 (construct T120.myc.TM5^T), two P-reactive fragments were recovered after PK digestion that contained 10% of the signal intensity and two-thirds of the initial methionine residues (Figure 4A, lanes 10–12). Thus, the reporter was translocated into the ER lumen by TM5, although reinitiation of translocation (~15%) was significantly less efficient than in XO. In these chains, TM5 and TM6 each spanned the membrane in their predicted orientations, and the TM5-TM6 peptide loop resided in the ER lumen. In contrast to XO, the myc epitope remained cytosolic and protease accessible in >90% of all constructs, including full-length AQP1 (compare Figure 4A, lanes 7–9 and 13–15, with Figure 3). These findings demonstrate that RRL supplemented with CRM failed to reorient the TM3-TM4 peptide loop and generate a mature six-spanning AQP1 topology. Consistent with this finding,

AQP1.T120.myc also failed to acquire its protease-resistant core conformation.

To understand the basis for the different AQP1 topologies in XO and RRL, we attempted to reconstitute AQP1 maturation with the use of a complementation approach. In this regard, supplementation of RRL with oocyte cytosol and microinjection of CRM containing in vitro synthesized AQP1 constructs into XO did not significantly improve AQP1 maturation efficiency (our unpublished results). However, when AQP1 constructs were expressed in RRL supplemented with XO-derived ER membranes (XOmb), myc-tagged constructs yielded a topology closely resembling that obtained from intact XO (Figure 4B). After synthesis of TM4 (T120.myc.TM4^T), the P reporter remained cytosolic, whereas the myc epitope became protected from PK in 27% of nascent chains (Figure 4B, lanes 1–6). (Note that the

16-kDa myc-reactive fragment represents only 9% of the initial signal intensity.) After synthesis of TM5 (T120.myc.TM5^T), 16% of nascent chains were again fully protected from protease (Figure 4B, lanes 7–12), and a PK-protected ~30-kDa fragment was recovered that contained both myc and P epitopes. As we had observed in oocytes, the myc epitope was protected from protease in a total of 34% of nascent chains at this stage of synthesis, and this fraction correlated well with the translocation efficiency of the P reporter (31%). Similarly, after synthesis of TM6, the P reporter and the AQP1 C terminus were cytosolic, whereas myc-reactive protease-protected fragments were recovered from 60% of T120.myc.TM6^T and 42% of AQP1.T120.myc nascent chains (Figure 4B, lanes 13–15 and 19–21). These data indicate that in XOmb, as in intact XO, reorientation of TM3 begins after synthesis of TM4 and that the efficiency of reorientation increases as additional C-terminal TM segments are synthesized.

In Vivo and In Vitro AQP1 Maturation

To determine whether the incomplete reorientation of TM3 in microinjected XO and in vitro expression systems represented an inefficient process versus delayed kinetics of maturation, we examined the topological maturation of full-length myc-tagged AQP1 constructs with the use of pulse-chase analysis. Two hours after RNA injection into XO, AQP1.T120.myc was recovered primarily as a core-glycosylated polypeptide with an apparent size of 33 kDa. PK digestion generated a 29- to 30-kDa myc-reactive fragment that contained 32% of the initial radioactive signal and 66% of the initial methionine residues. Thus, 48% of newly synthesized AQP1 protein achieved a protease-resistant conformation immediately after synthesis (Figure 5, A and F). During the chase period, we observed a small but reproducible increase in both the fraction and the absolute amount of core-glycosylated AQP1 protein that acquired a protease-protected conformation. Protease protection of the myc epitope reached a maximum value of 78% within 5 h of synthesis (average of three experiments; Figure 5F).

In contrast to XO, <10% of AQP1.T120.myc acquired a protease-resistant conformation in RRL supplemented with CRM within 1 h (Figure 5B, lanes 1–3). This fraction increased to only 23% during the 12-h chase (Figure 5B, lanes 4–12, and 5F). For these experiments, CRM were >95% efficient at directing polypeptide translocation, and the integrity of the microsomal membranes remained completely intact during the chase period (Figure 5C). Additional experiments demonstrated that AQP1 maturation efficiency was not significantly altered in RRL when translation and/or incubation was carried out at different temperatures (our unpublished results). In RRL supplemented with XOmb, 34% and 75% of glycosylated AQP1.T120.myc acquired a protease-resistant conformation within 1 and 12 h, respectively (Figure 5, D and F). RRL supplemented with XOmb thus exhibited similar efficiency in promoting AQP1 topological maturation as intact oocytes. Translocation was also efficient in XOmb, and membrane integrity was maintained during the entire incubation period (Figure 5E). Thus, failure of AQP1 to mature in CRM was not simply an artifact of the in vitro RRL system but rather reflected specific properties of ER-derived microsomal membranes. Importantly, the efficiency of different ER membranes to direct transloca-

tion did not appear to predict their ability to reconstitute additional events required for AQP1 topological maturation.

To rule out the possibility that the increase in myc epitope protection might be due to a relative instability of the four-spanning structure, total AQP1 protein was quantitated for each time point (Figure 5G). In each system, a gradual loss of protein was noted. However, degradation was slow and occurred over a period that would not explain the observed change in topology. In both XO and XOmb, >90% of AQP1 was present 5 h after synthesis, at a time when reorientation was nearly complete.

Immunoabsorption of AQP1 in ER-derived Membranes

To further confirm that the T120-myc epitope was translocated into the ER lumen during in vitro AQP1 maturation, we tested the cytosolic accessibility of the myc epitope with the use of a nonproteolytic immunoabsorption assay (Figure 6). Full-length AQP1 constructs, AQP1.T120.myc, and a control protein encoding an N-terminal myc tag (myc.AQP1) were expressed in RRL supplemented with CRM or XOmb. Microsomes were incubated in the presence or absence of anti-myc antibody and pelleted through a sucrose cushion. Protein recovered by adsorbed antibody was then compared with protein recovered by immunoprecipitation after detergent solubilization. Immunoabsorption of the control protein containing an N-terminal myc epitope was >50% in both CRM and XOmb (Figure 6, A and C). This result is consistent with the established cytosolic orientation of the N terminus (Smith and Agre, 1991; Skach *et al.*, 1994) and demonstrates that the myc tag on membrane-bound protein is accessible to cytosolic antibody. Less than 10% of immunoprecipitated protein was recovered by immunoabsorption when the myc epitope was located in the ER lumen (at residue P77; our unpublished results). In CRM, the immunoabsorption efficiency of the AQP1.T120.myc construct was 55 and 45% within 1 and 8 h of translation, respectively, indicating that the myc epitope at residue T120 remained predominantly accessible from the cytosol, as would be expected in the four-spanning topology illustrated in Figure 1. In XOmb, however, the efficiency of immunoabsorption was initially only 23%, and this decreased to 13% after 8 h of incubation, consistent with repositioning of the myc epitope into an inaccessible, luminal location (Figure 6, B and C). More than 80% of total AQP1 protein was recovered within the 8-h incubation period. These findings support conclusions from proteolysis experiments that XOmb, but not CRM, efficiently reconstitute translocation of the T120-myc epitope into the ER lumen.

Topological Reorientation of TM3 Involves Retrograde Translocation of N-terminal Flanking Residues

If AQP1 were converted from its four-spanning to its six-spanning topology by a 180-degree rotation of TM3, then as TM3 C-terminal residues translocated into the ER lumen, TM3 N-terminal residues would be predicted to move from the ER lumen to the cytosol. We tested this hypothesis using the AQP1.P77.myc construct. Studies of sequentially truncated P77 myc constructs indicated that the myc tag did not significantly alter the cotranslational activities of down-

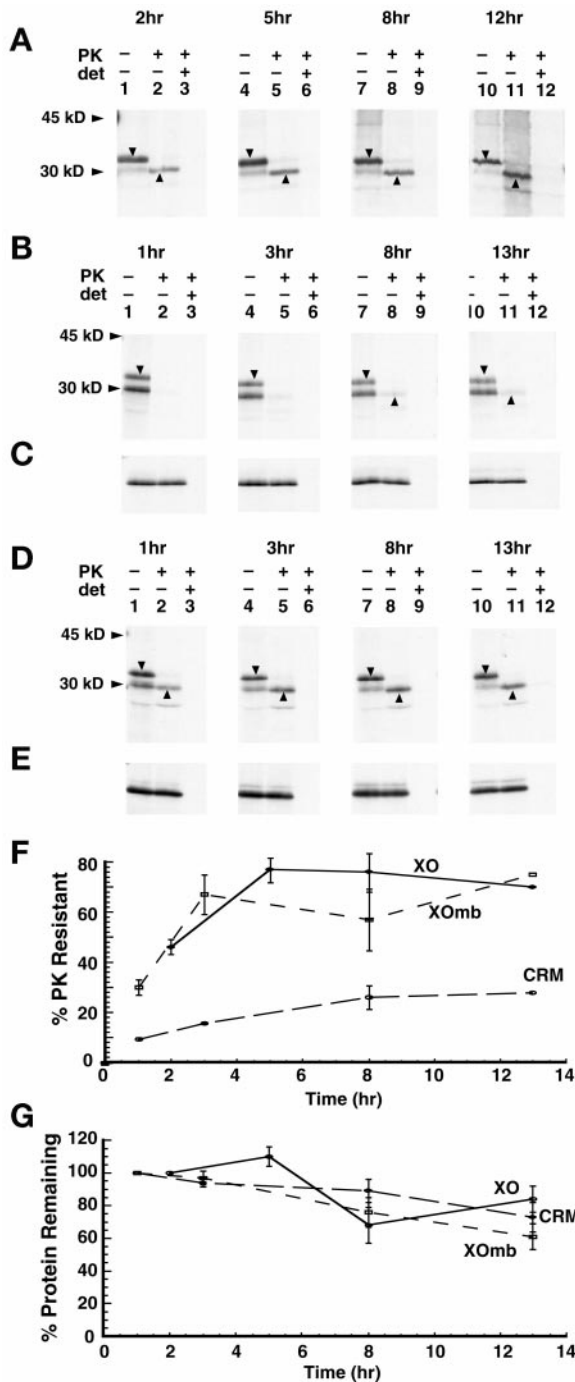


Figure 5. Topological maturation of AQP1 in vivo and in vitro. Plasmids encoding AQP1.T120.myc were expressed in microinjected *Xenopus* oocytes (A), RRL supplemented with CRM (B), and RRL supplemented with ER-derived oocyte ER membranes (D) as described in MATERIALS AND METHODS. At the times indicated after RNA injection (A) or the initiation of in vitro translation (B–E), samples were digested with PK and immunoprecipitated as in Figures 3 and 4. Downward arrowheads indicate glycosylated full-length AQP1 chains. Upward arrowheads indicate the PK-protected AQP1 hydrophobic core. C and E show protease protection results of the secretory control protein, bovine prolactin, translated and

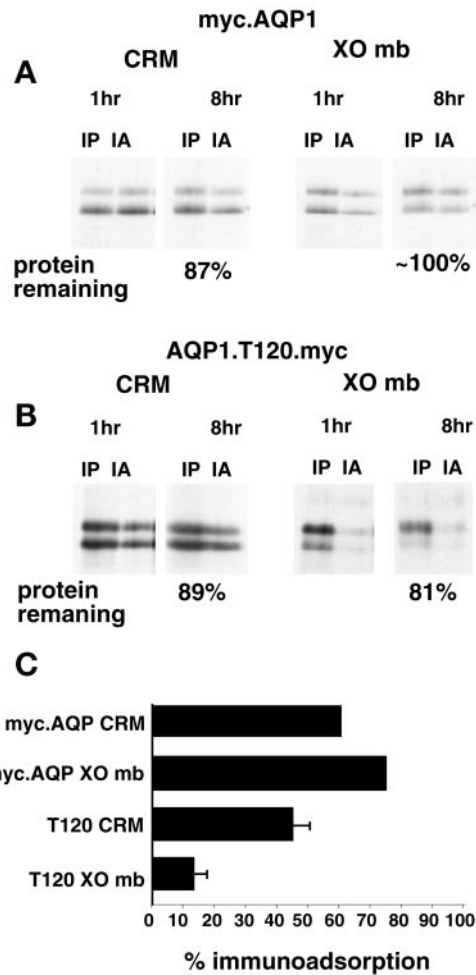


Figure 6. Immunoabsorption of myc-tagged AQP1. Plasmids encoding the myc epitope at residue M1, myc.AQP1 (A), or residue T120, AQP1.T120.myc (B), were translated in RRL in the presence of CRM or XOmb for 1 h. After translation, immunoabsorption (IA) and immunoprecipitation (IP) were performed as described in MATERIALS AND METHODS. (C) Percent protein recovered by immunoabsorption relative to protein recovered by immunoprecipitation after the 8-h chase period. Total protein remaining at 8 h is indicated beneath the autoradiograms. Values indicate the average of two experiments for the control plasmid, myc.AQP1, and three experiments (\pm SE) for AQP1.T120.myc.

stream topogenic determinants encoded within TMs 4, 5, and 6 (our unpublished results). However, as noted above, these constructs were poorly expressed in XO. Therefore, we determined their topology in RRL supplemented with either CRM or XOmb.

PK digestion of the full-length AQP1.P77.myc construct resulted in the appearance of two protease-protected, myc-

incubated in CRM and XOmb, respectively. (F) Protease resistance of AQP1.T120.myc was determined by the fraction of glycosylated chains that had acquired PK resistance. (G) Total AQP protein at each time point. Results represent the average of three to four separate experiments \pm SE.

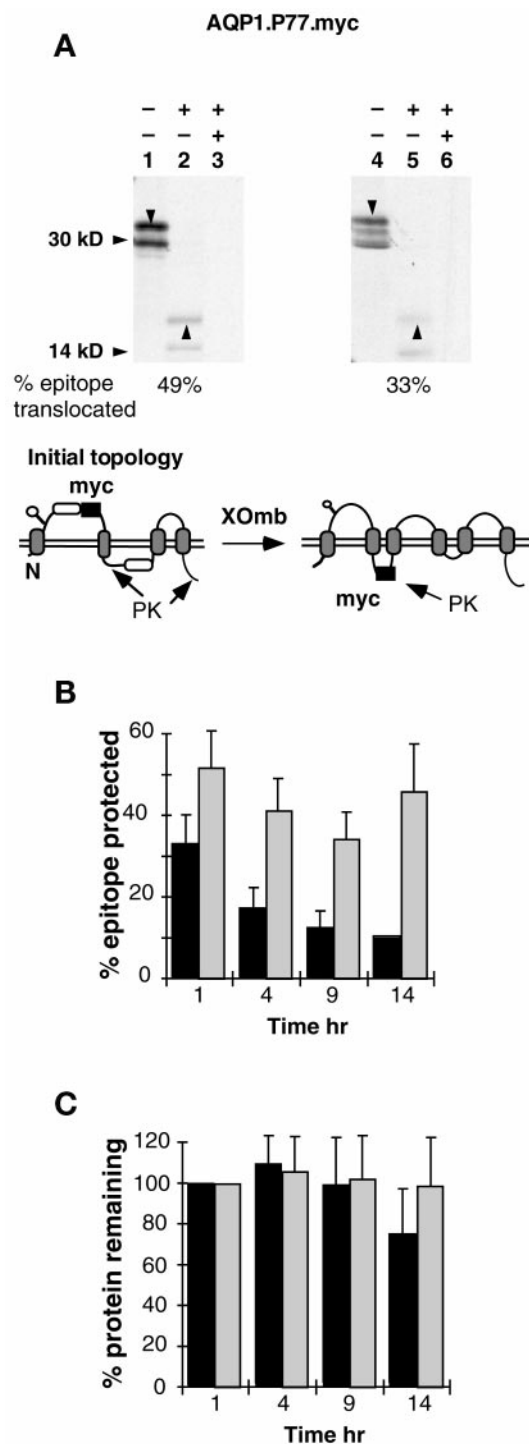


Figure 7. Topological reorientation of TM3 N-terminal flanking residues. (A) AQP1.P77.myc expressed in RRL supplemented with CRM (lanes 1–3) or XOmb (lanes 4–6) was digested with PK and immunoprecipitated with anti-myc antibody as in Figure 4. Downward arrowheads indicate full-length core-glycosylated AQP1 constructs. Upward arrowheads indicate glycosylated myc-reactive fragments derived from full-length polypeptides. The diagram shows the orientation of the myc epitope that would give rise to the

reactive fragments (Figure 7A). The size of the larger 19-kDa fragment (corrected for the myc epitope) corresponded precisely with the translocated and glycosylated N-terminal peptide loop previously shown to contain TM1, TM2, and TM3 in the four-spanning AQP1 topology (Skach *et al.*, 1994). After adjusting for methionine content, the average translocation efficiency of the myc epitope in full-length glycosylated chains was 53% in CRM ($n = 6$) and 33% in XOmb ($n = 4$) (Figure 7B). In addition, the myc epitope became progressively more accessible to PK in XOmb after translation (87% accessible after 14 h), whereas accessibility remained essentially unchanged in CRM. No significant difference in AQP1 stability was observed between different membrane preparations (Figure 7C). The efficiency and kinetics of reorientation differed somewhat from the T120.myc-tagged constructs. This may be due to other effects of the myc tag on AQP1 folding, because AQP1.P77.myc does not form functional water channels. Together with data from the T120 myc constructs, these findings support a model in which AQP1 topological maturation involves a coordinated repositioning of TM3 N-terminal and C-terminal flanking residues to opposite sides of the ER membrane.

DISCUSSION

It is generally accepted that the topology of most eukaryotic polytopic proteins is established cotranslationally at the ER membrane and once established is maintained during subsequent steps of processing and intracellular trafficking. The current study provides an exception to this rule and demonstrates that initial cotranslational topology at the ER membrane is dynamic and may be modified by subsequent folding events. Specifically, AQP1 maturation proceeds through a complex pathway that involves posttranslational reorientation of three internal TM segments and two connecting peptide loops. Initial translocation events are cotranslationally directed by sequential signal and stop-transfer sequences and give rise to a loosely folded, protease-sensitive, four-spanning structure (Skach *et al.*, 1994). During subsequent maturation, TM3 C-terminal flanking residues are posttranslationally reoriented from an initial PK-accessible location in the cytosol to a PK-protected location in the ER lumen. Concurrently, TM3 N-terminal flanking residues undergo a retrograde translocation from the ER lumen to the cytosol. We propose that these events are associated with a 180-degree rotation of TM3 into its mature type II topology and a repositioning of TM2 and TM4 within the plane of the membrane to generate the predicted six-spanning AQP1 structure, as diagrammed in Figure 1. Although TM3 reorientation was initially detected after synthesis of TM4 and TM5, the efficiency of reorientation was significantly en-

protected fragment(s). (B) Pulse-chase analysis of AQP1.P77.myc expressed in RRL supplemented with CRM (hatched bars) or XOmb (solid bars) was performed as in Figure 5. The percent epitope protected represents the fraction of full-length glycosylated chains that gave rise to the 19-kDa myc-reactive, PK-protected fragments. Translocation values are corrected for methionine content and represent the average of six (CRM) or two to four (XOmb) experiments. (C) Total protein was averaged from seven (CRM) or five (XOmb) experiments and normalized for protein present at 1 h (\pm SE).

hanced after synthesis of all six TM segments. In intact XO and in XOmb, AQP1 maturation was also associated with the acquisition of a protease-resistant core structure, suggesting that TM3 reorientation was accompanied by compaction of TM helices and/or cytosolic peptide loops in the final mature and functional protein.

These findings have significant implications for the molecular mechanisms by which polytopic proteins acquire their topology in the ER membrane. During eukaryotic protein synthesis, the immediate (i.e., cotranslational) topological fate of the nascent chain is primarily dependent on two factors: binding of ribosomes to the ER membrane, and the gated state of the Sec61 translocation channel (Crowley *et al.*, 1994; Do *et al.*, 1996; Liao *et al.*, 1997; Mothes *et al.*, 1997). As the nascent chain exits the ribosome, it either moves through the translocation channel toward the ER lumen or exits the ribosome in direct contact with the cytosol (Crowley *et al.*, 1994; Jungnickel and Rapoport, 1995; Liao *et al.*, 1997; Hamman *et al.*, 1998). By precisely regulating the state of ribosome binding and translocon gating, signal and stop-transfer sequences in polytopic proteins are able to control the environment encountered by the growing nascent chain and establish polytopic protein topology in a cotranslational manner (Bibi, 1998). Initial events of AQP1 biogenesis, therefore, are partially explained by the action of signal sequence activities encoded within TM1 and TM5 and stop-transfer activities encoded within TM3 and TM6 (Skach *et al.*, 1994). The surprising outcome here is that AQP1 acquires only four membrane-spanning segments through these cotranslational events (Skach *et al.*, 1994). In particular, TM2 is unable to terminate translocation (Skach *et al.*, 1994) and transiently resides within the ER lumen, whereas TM3 terminates translocation and initially spans the membrane in an orientation opposite that observed in the mature protein (Preston *et al.*, 1994).

AQP1 maturation, therefore, requires a novel mechanism for reorienting TM segments (e.g., TM3) that have achieved an intermediate transmembrane topology. It is possible that TM3 reorientation could occur after the nascent chain has been released from the translocon and during helical packing (Popot and Engelman, 1990). Such a process seems unlikely, however, because it would require that polar and charged residues traverse the hydrophobic environment of the membrane. Rather, AQP1 topological maturation appears to be initiated while the nascent chain is still associated with the Sec61 translocation machinery and/or other ER proteins. In this regard, carbonate extraction experiments have indicated that the nascent AQP1 chain is unable to integrate stably into the ER membrane until at least three TM segments have been synthesized (Skach *et al.*, 1994). In the current study, TM3 reorientation appears to begin even before AQP1 synthesis is completed, at a time when the ribosome would be expected to remain bound to Sec61 (Borel and Simon, 1996; Mothes *et al.*, 1997). This finding is consistent with the large internal diameter of the translocon pore (20–60 Å) (Hanein *et al.*, 1996; Hamman *et al.*, 1997) as well as with recent studies suggesting that TM segments may accumulate within or near the translocon before entering the lipid bilayer (Skach and Lingappa, 1993; Lin and Addison, 1995; Borel and Simon, 1996; Mothes *et al.*, 1997). It is thus possible that ER translocation machinery might potentially hold AQP1 N-terminal TM segments in an interme-

mediate folded state until synthesis of downstream TM segments provides sufficient information to allow the completion of folding and membrane integration of all helices (Hegde and Lingappa, 1997). The absence of this downstream folding information could explain why truncated constructs such as T120.myc.TM5^T inefficiently acquired a protease-resistant core conformation and exhibited multiple intermediate topological forms.

The possibility that translocon-associated proteins might play an active role in facilitating polytopic protein folding raises several questions. How might the exit of TM segments from the translocon be monitored and regulated during polytopic protein biogenesis? How would the accumulation of TM helices affect or be affected by translocon gating? And how might retrograde and anterograde translocation of peptide segments be facilitated? Further studies examining the molecular environment of individual TM helices at specific stages of biogenesis will be required to address these issues.

C-terminal translocation reporters have been widely used to study polytopic protein topology and rely on the ability of upstream topogenic information to accurately direct the topology of downstream polypeptide segments (Traxler *et al.*, 1993). Moreover, this technique assumes that the initial topology of a protein in the ER membrane accurately reflects the topology of the protein elsewhere in the cell. Based on this premise, we previously proposed that the four-spanning AQP1 topology might represent a functional water channel unit (Skach *et al.*, 1994). It appears, however, that this four-spanning structure is actually a folding intermediate of AQP1 maturation. Thus, although the C-terminal reporter technique provides valuable insight into the process of protein biogenesis, it may or may not accurately predict final topology depending on whether posttranslational topological modifications occur. It should be noted that translocation events can also be influenced by both the presence of the reporter and the choice of the fusion site. To reduce this possibility, we have used a reporter domain that faithfully and passively follows a wide variety of heterologous topogenic signals (Rothman *et al.*, 1988; Chavez and Hall, 1992). Moreover, examination of homologous fusion proteins derived from a closely related aquaporin, AQP4, and use of the same reporter and similar fusion sites suggest that specific structural information within TM2 and TM3 is responsible for the unusual biogenesis pathway observed for AQP1 (Shi *et al.*, 1995).

A growing number of eukaryotic proteins have recently been recognized to exhibit variations in cotranslational biogenesis pathways. Frequently, these variations involve local interactions between adjacent topogenic determinants. For example, C-terminal TM segments have been observed to facilitate the translocation and positioning of adjacent N-terminal TM segments, particularly those TM segments that are relatively short or that contain charged residues (Calamia and Manoil, 1992; Wilkinson *et al.*, 1996; Bayle *et al.*, 1997; Lu *et al.*, 1997; Schmidt-Rose and Jentsch, 1997; Ota *et al.*, 1998). In the case of AQP1, topological maturation involves more global aspects of protein folding in which distal structural elements influence anterograde as well as retrograde translocation events. AQP1 biogenesis thus resembles that of Sec61p, in which the C-terminal half of the protein was required to facilitate the proper transmembrane orientation of the N-terminal half (Wilkinson *et al.*, 1996). Nonco-

translational biogenesis pathways, therefore, may explain in part why different topological models have been obtained when the results of C-terminal reporters are compared with other analytical techniques (Adachi *et al.*, 1994; Doan *et al.*, 1996; Schmidt-Rose and Jentsch, 1997; Li and Greenwald, 1998; Nakai *et al.*, 1999).

It is important to note that some aspects of protein topology may be expression system dependent. Canine pancreatic microsomes were remarkably inefficient at reconstituting TM3 reorientation, even though they were nearly 100% efficient at directing translocation of a secretory protein. In contrast, AQP1 topological maturation was efficiently observed in both intact XO and oocyte-derived ER membranes. A similar result was reported previously by Kobilka (1990), who found that XOmb but not CRM were able to confer substrate-binding properties and protease resistance to *in vitro* translated β -adrenergic receptor. One intriguing possibility is that certain polytopic proteins may require specialized components to achieve their proper topology in addition to the basic components needed for protein translocation (Hegde *et al.*, 1998; Hegde and Lingappa, 1999). Differences between CRM and XOmb in mediating AQP1 maturation, therefore, might reflect different amounts of translocation-associated factors in different cell types. It is also possible that differences in AQP1 maturation are due to different techniques of membrane preparation or, alternatively, other aspects of biogenesis, such as tetramerization (Smith and Agre, 1991; Ma *et al.*, 1993). Finally, although oocytes efficiently generate functional aquaporins, it is unclear whether AQP biogenesis in mammalian cells might exhibit yet additional folding variations. Further studies defining how different ER membrane preparations mediate AQP1 maturation will undoubtedly provide insight into these unique aspects of polytopic protein biogenesis.

ACKNOWLEDGMENTS

The authors are grateful to members of the Skach laboratory for helpful discussions and critical comments on the manuscript, and to K. Moss for technical assistance. This work was supported by National Institutes of Health grants GM 53457 and DK51818. W.R.S. is an established investigator of the American Heart Association.

REFERENCES

- Adachi, S., Uchida, S., Ito, H., Hata, M., Hiroe, M., Marumo, F., and Sasaki, S. (1994). Two isoforms of a chloride channel predominantly expressed in thick ascending limb of Henle's loop and collecting ducts of rat kidney. *J. Biol. Chem.* 269, 17677–17683.
- Agre, P., Bonhivers, M., and Borgnia, M.J. (1998). The aquaporins, blueprints for cellular plumbing systems. *J. Biol. Chem.* 273, 14659–14662.
- Audigier, Y., Friedlander, M., and Blobel, G. (1987). Multiple topogenic sequences in bovine opsin. *Proc. Natl. Acad. Sci. USA* 84, 5783–5787.
- Bayle, D., Weeks, D., and Sachs, G. (1997). Identification of membrane insertion sequences of the rabbit gastric cholecystokinin-A receptor in *in vitro* translation. *J. Biol. Chem.* 272, 19697–19707.
- Beja, O., and Bibi, E. (1995). Multidrug resistance protein (Mdr)-alkaline phosphatase hybrids in *Escherichia coli* suggest a major revision in the topology of the C-terminal half of Mdr. *J. Biol. Chem.* 270, 12351–12354.
- Bibi, E. (1998). The role of the ribosome-translocon complex in translation and assembly of polytopic membrane proteins. *Trends Biochem. Sci.* 23, 51–55.
- Blobel, G. (1980). Intracellular protein topogenesis. *Proc. Natl. Acad. Sci. USA* 77, 1496–1500.
- Borel, A., and Simon, S. (1996). Biogenesis of polytopic membrane proteins: Membrane segments assemble within translocation channels prior to membrane integration. *Cell* 85, 379–389.
- Boyd, D., Manoil, C., Froshauer, S., Millan, J., Green, N., McGovern, K., Lee, C., and Beckwith, J. (1990). Use of Gene Fusions to Study Membrane Protein Topology, Washington, DC: American Association for the Advancement of Science.
- Broome-Smith, J., Tadayyon, M., and Zhang, Y. (1990). Beta-lactamase as a probe of membrane protein assembly and protein export. *Mol. Microbiol.* 4, 1637–1644.
- Calamia, J., and Manoil, C. (1992). Membrane protein spanning segments as export signals. *J. Mol. Biol.* 224, 539–543.
- Chavez, R., and Hall, Z. (1992). Expression of fusion proteins of the nicotinic acetylcholine receptor from mammalian muscle identifies the membrane-spanning regions in the alpha and delta subunits. *J. Cell Biol.* 116, 385–393.
- Cheng, A., van Hoek, A.N., Yeager, M., Verkman, A.S., and Mitra, A.K. (1997). Three-dimensional organization of a human water channel. *Nature* 387, 627–630.
- Crowley, K., Liao, S., Worrell, V., Reinhart, G., and Johnson, A. (1994). Secretory proteins move through the endoplasmic reticulum membrane via an aqueous, gated pore. *Cell* 78, 461–471.
- Do, H., Falcone, D., Lin, J., Andrews, D., and Johnson, A. (1996). The cotranslational integration of membrane proteins into the phospholipid bilayer is a multistep process. *Cell* 85, 369–378.
- Doan, A., *et al.* (1996). Protein topology of presenilin 1. *Neuron* 17, 1023–1030.
- Evan, G., Lewis, G., Ramsay, G., and Bishop, J.M. (1985). Isolation of monoclonal antibodies specific for human c-myc proto-oncogene product. *Mol. Cell. Biol.* 5, 3610–3616.
- Hamman, B., Chen, J.-C., Johnson, E., and Johnson, A. (1997). The aqueous pore through the translocon has a diameter of 40–60 Å during cotranslational protein translocation at the ER membrane. *Cell* 89, 535–544.
- Hamman, B., Hendershot, L., and Johnson, A. (1998). BiP maintains the permeability barrier of the ER membrane by sealing the luminal end of the translocon pore before and early in translocation. *Cell* 92, 747–758.
- Hanein, D., Matlack, K., Jungnickel, B., Plath, K., Kalies, K.U., Miller, K., Tapoport, T., and Akey, C. (1996). Oligomeric rings of the Sec61p complex induced by ligands required for protein translocation. *Cell* 87, 721–732.
- Hasegawa, H., Ma, T., Skach, W., Matthey, M., and Verkman, A. (1994). Molecular cloning of a mercurial-insensitive water channel expressed in selected water-transporting tissues. *J. Biol. Chem.* 269, 5498–5500.
- Hegde, R., and Lingappa, V. (1997). Membrane protein biogenesis: regulated complexity at the endoplasmic reticulum. *Cell* 91, 675–682.
- Hegde, R., and Lingappa, V. (1999). Regulation of protein biogenesis at the endoplasmic reticulum membrane. *Trends Cell Biol.* 9, 132–137.
- Hegde, R., Voigt, S., and Lingappa, V. (1998). Regulation of protein topology by trans-acting factors at the endoplasmic reticulum. *Mol. Cell* 2, 85–91.
- Ho, N., Hunt, H., Horton, R., Pullen, J., and Pease, P. (1989). Site-directed mutagenesis by overlap extension using the polymerase chain reaction. *Gene* 77, 51–59.

- Johnson, A. (1997). Protein translocation at the ER membrane: a complex process becomes more so. *Trends Cell Biol.* 7, 90–94.
- Jungnickel, B., and Rapoport, T. (1995). A posttargeting signal sequence recognition event in the endoplasmic reticulum membrane. *Cell* 82, 261–270.
- Kobilka, B. (1990). The role of cytosolic and membrane factors in processing of the human beta-2 adrenergic receptor following translocation and glycosylation in a cell free system. *J. Biol. Chem.* 265, 7610–7618.
- Li, X., and Greenwald, I. (1998). Additional evidence for an eight-transmembrane-domain topology for *Caenorhabditis elegans* and human presenilins. *Proc. Natl. Acad. Sci. USA* 95, 7109–7114.
- Liao, S., Lin, J., Do, H., and Johnson, A. (1997). Both luminal and cytosolic gating of the aqueous translocon pore are regulated from inside the ribosome during membrane protein integration. *Cell* 90, 31–42.
- Lin, J., and Addison, R. (1995). A novel integration signal that is composed of two transmembrane segments is required to integrate the *Neurospora* plasma membrane H⁺-ATPase into microsomes. *J. Biol. Chem.* 270, 6935–6941.
- Lipp, J., Flint, N., Haeuptle, M.T., and Dobberstein, B. (1989). Structural requirements for membrane assembly of proteins spanning the membrane several times. *J. Cell Biol.* 109, 2013–2022.
- Lu, Y., Xiong, X., Bragin, A., Kamani, K., and Skach, W. (1997). Co- and posttranslational mechanisms direct CFTR N-terminus transmembrane assembly. *J. Biol. Chem.* 273, 568–576.
- Ma, T., Frigeri, A., Tsai, S.-T., Verbavatz, J., and Verkman, A.S. (1993). Localization and functional analysis of CHIP28 water channels in stably transfected CHO cells. *J. Biol. Chem.* 268, 22756–22764.
- Mothes, W., Heinrich, S., Graf, R., Nilsson, I., von Heijne, G., Brunner, J., and Rapoport, T. (1997). Molecular mechanism of membrane protein integration into the endoplasmic reticulum. *Cell* 89, 523–533.
- Nakai, T., Yamasaki, A., Sakaguchi, M., Kosaka, K., Mihara, K., Amaya, Y., and Miura, S. (1999). Membrane topology of Alzheimer's disease-related presenilin 1. *J. Biol. Chem.* 274, 23647–23658.
- Ota, K., Sakaguchi, M., von Heijne, G., Hamasaki, N., and Mihara, K. (1998). Forced transmembrane orientation of hydrophilic polypeptide segments in multispinning membrane proteins. *Mol. Cell* 2, 495–503.
- Popot, J.L., and Engelman, D. (1990). Membrane protein folding and oligomerization: the two stage model. *Biochemistry* 29, 4031–4037.
- Preston, G., Jung, J., Guggino, W., and Agre, P. (1994). Membrane topology of aquaporin CHIP: analysis of functional epitope-scanning mutants by vectorial proteolysis. *J. Biol. Chem.* 269, 1668–1673.
- Preston, G.M., and Agre, P. (1991). Isolation of the cDNA for erythrocyte integral membrane protein of 28-kilodaltons: member of an ancient channel family. *Proc. Natl. Acad. Sci. USA* 88, 11110–11114.
- Preston, G.M., Carroll, T.P., Guggino, W.B., and Agre, P. (1992). Appearance of water channels in *Xenopus* oocytes expressing red cell CHIP28 protein. *Science* 256, 385–387.
- Rapoport, T., Rolls, M., and Jungnickel, B. (1996). Approaching the mechanism of protein transport across the ER membrane. *Curr. Opin. Cell Biol.* 8, 499–504.
- Rothman, R.E., Andrews, D.W., Calayag, M.C., and Lingappa, V.R. (1988). Construction of defined polytopic integral transmembrane proteins. *J. Biol. Chem.* 263, 10470–10480.
- Schmidt-Rose, T., and Jentsch, T.J. (1997). Transmembrane topology of a CLC chloride channel. *Proc. Natl. Acad. Sci. USA* 94, 7633–7638.
- Shi, L.-B., Skach, W., Ma, T., and Verkman, A. (1995). Distinct biogenesis mechanisms for water channels MIWC and CHIP28 at the endoplasmic reticulum. *Biochemistry* 34, 8250–8256.
- Simon, S.M., and Blobel, G. (1991). A protein-conducting channel in the endoplasmic reticulum. *Cell* 65, 371–380.
- Skach, W. (1998). *Topology of P-Glycoproteins*. San Diego: Academic Press.
- Skach, W., and Lingappa, V. (1993). Amino terminus assembly of human P-glycoprotein at the endoplasmic reticulum is directed by cooperative actions of two internal sequences. *J. Biol. Chem.* 268, 23552–23561.
- Skach, W., and Lingappa, V. (1994). Transmembrane orientation and topogenesis of the 3rd and 4th membrane-spanning regions of human P-glycoprotein (MDR1). *Cancer Res.* 54, 3202–3209.
- Skach, W., Shi, L.-B., Calayag, M.C., Frigeri, A., Lingappa, V., and Verkman, A. (1994). Biogenesis and transmembrane topology of the CHIP28 water channel in the endoplasmic reticulum. *J. Cell Biol.* 125, 803–815.
- Smith, B.L., and Agre, P. (1991). Erythrocyte M_r 28,000 transmembrane protein exists as a multisubunit oligomer similar to channel proteins. *J. Biol. Chem.* 266, 6407–6415.
- Traxler, B., Boyd, D., and Beckwith, J. (1993). The topological analysis of integral cytoplasmic membrane proteins. *J. Membr. Biol.* 132, 1–11.
- Verkman, A., van Hoek, A., Ma, T., Frigeri, A., Skach, W., Mitra, A., Tamarappoo, B., and Farinas, J. (1996). Water transport across mammalian cell membranes. *Am. J. Physiol.* 270, C12–C30.
- Walter, P., and Blobel, G. (1983). *Preparation of Microsomal Membranes for Cotranslational Protein Translocation*. New York: Academic Press.
- Walz, T., Hiram, T., Murata, K., Heymann, J.B., Mitsuoka, K., Fujiyoshi, Y., Smith, B.L., Agre, P., and Engel, A. (1997). The three-dimensional structure of aquaporin-1. *Nature* 387, 624–627.
- Wessels, H., and Spiess, M. (1988). Insertion of a multispinning membrane protein occurs sequentially and requires only one signal sequence. *Cell* 55, 61–70.
- Whale, S., and Stoffel, W. (1996). Membrane topology of the high-affinity L-glutamate transporter (GLAST-1) of the central nervous system. *J. Cell Biol.* 135, 1867–1877.
- Wilkinson, B., Critchley, A., and Stirling, C. (1996). Determination of the transmembrane topology of yeast Sec61p, an essential component of the endoplasmic reticulum translocation complex. *J. Biol. Chem.* 271, 25590–25597.
- Xiong, X., Bragin, A., Widdicombe, J., Cohn, J., and Skach, W. (1997). Structural cues involved in ER degradation of G85E and G91R mutant CFTR. *J. Clin. Invest.* 100, 1079–1088.
- Yost, C.S., Hedgpeth, J., and Lingappa, V.R. (1983). A stop transfer sequence confers predictable transmembrane orientation to a previously secreted protein in cell-free systems. *Cell* 34, 759–766.
- Zhang, R., and Verkman, A.S. (1991). Water and urea transport in *Xenopus* oocytes: expression of mRNA from toad urinary bladder. *Am. J. Physiol.* 260, 26–34.